

# MPC-based centralised power control in EV charging station with battery storage system and PV coordination

Messilem A.Mohamed<sup>1</sup> and Ruggero Carli<sup>2</sup> and Sandro Zampieri<sup>2</sup>

**Abstract**—This work presents a study on the optimal control of an electric vehicle (EV) charging station, with a dual objective of minimizing operational expenses and accommodating EV owner preferences. The control frame work employs Model Predictive Control (MPC) to efficiently distribute power among the stations components, encompassing photovoltaic panel (PV), and energy storage system (ESS) battery, the grid connection, and connected EVs. Our MPC scheme takes into account EV owner requirements, with owners providing information about their charging needs (required energy) and departure times when plugging in their vehicles. With this extra information that helps energy management of the system, we exploited the integration of Vehicle-to-Grid (V2G) technology, enabling bidirectional power flow to and from grid. This feature allows EVs to supply electricity to the grid during periods of high demand or when solar energy generation is insufficient. The proposed MPC-based method is validated through simulation and compared with heuristic method that disregards owner information and tends to charge EV at maximum power rate available. This comparative analysis serves to evaluate the efficacy of the proposed approach in terms of cost savings, good energy management, and owner satisfaction.

## I. INTRODUCTION

The targets of the 2030 UN's Agenda for Sustainable Development related to ensuring access to affordable, sustainable, and modern energy are aligned with the global effort to address climate change, to promote clean energy, and to achieve sustainable development [1]. Smart grids integrate renewable energy sources (RESs) like solar and wind power by forecasting their output and coordinating with conventional generation, ensuring stable power supply. They also enable the integration of energy storage systems (ESS) to capture and release excess electricity as needed.

Electric vehicles (EV) have gained immense popularity due to their environmental benefits and reduced dependency on fossil fuels [2], [3]. EVs can be charged using various methods, including standard AC charging from the power grid or fast DC charging stations [4]. However, concerns

have been raised about the peak power requirements for recharging EV batteries. Indeed, some people are worried that the existing electrical infrastructure might not be able to handle the simultaneous demand electricity during peak charging periods [5]. Demand response (DR) was already recognised as a crucial mechanism in the coordination of energy production and consumption, especially with the increasing adoption of renewable energy sources and the growth of prosumers [6], [7]. In the context of prosumers, demand response becomes even more significant. Prosumers can generate excess of electricity when their renewable energy sources produce more than their own consumption needs. Instead of wasting this surplus energy or feeding it back into the grid at times when it might not be needed, demand response mechanisms allow prosumers to respond to market signals and adjust their consumption or sell the excess of energy to the grid when electricity prices are high [8]. An efficient management system for prosumers requires the development and implementation of advanced control strategies that enhance demand flexibility and minimize economic expenditures [9]. In this context, model predictive control (MPC) is being considered as a promising control strategy for efficiently managing users resources [10]. It is particularly well-suited for systems with constraints and dynamic behaviour, making it an effective approach for managing resources in various applications [11], [12].

In this paper, we employ a model predictive control (MPC) approach for the management of a station featuring a specific number of EVs chargers, a photovoltaic (PV) power source, an energy storage system, and a connection to the upstream grid. The MPC architecture takes into account the predicted EVs arrivals, including data on the arrival time, departure time, and the associated energy requirements. Furthermore, it utilizes the real data when they become available; in particular, the departure time and energy requirement information are provided by the EV owner upon plugging in the vehicle. This additional information contribute to an enhanced energy management strategy as compared to a heuristic method where no owners' information is utilized and tends to charge EVs at maximum power rate available. The primary objective of our approach is to optimize the utilization of renewable energy from the PV source and energy storage system, all while ensuring that the EVs batteries are adequately charged.

The organization of the paper is as follows. In Section 2, we focus on detailing the system model and assumptions, providing a clear understanding of the power distribution system and the parameters considered in the MPC formulation. In Section 3, we describe the proposed energy man-

<sup>1</sup> Department of Information Engineering, University of Padova, Via Giovanni Gradenigo 6/B, 35131 Padova, Italy mohamedabdelm.messilem@studenti.unipd.it

<sup>2</sup> Department of Information Engineering, University of Padova, Via Giovanni Gradenigo 6/B, 35131 Padova, Italy carlirug@dei.unipd.it

<sup>3</sup> Department of Information Engineering, University of Padova, Via Giovanni Gradenigo 6/B, 35131 Padova, Italy zampi@dei.unipd.it

This study was carried out within the MOST-Sustainable Mobility Center and received funding from the European Union Next-GenerationEU (PIANO NAZIONALE DI RIPRESA E RESILIENZA (PNRR)-MISSIONE 4 COMPONENTE 2, INVESTIMENTO 1.4-D.D. 1033 17/06/2022, CN00000023). This manuscript reflects only the authors' views and opinions, neither the European Union nor the European Commission can be considered responsible for them.

agement system based on MPC. In Section 4, we outline the simulation setup, specifying the environment and parameters employed in the experiments and we provide numerical results comparing our MPC-based strategy to a conventional (heuristic) control. In section 5 we gather our conclusions.

## II. EV STATION SYSTEM MODELLING

In this paper we consider a EV charging station which is connected to the main distribution electric grid and is equipped with a PV source and a battery. The charging station acts as an energy supplier, providing the aggregate charging power for the EVs that arrive to it. The charging power is sourced from a combination of the PV production, the battery and the grid. In the next subsections we provide a modeling of the main components of the charging station. The models are in discrete-time and we assume that all the electric quantities are sampled by  $T_s$ .

### A. Battery Model

We assume that the battery has a maximum capacity energy  $E_b^{max}$ . Hence, the state of charge of the battery is:

$$SOC_b(k+1) = SOC_b(k) + P_b(k)T_s/E_b^{max}, \quad (1)$$

where  $SOC_b(k)$  is the state of charge of the battery at time  $kT_s$ . When the power is negative, it means that the battery is discharging, when the power is positive, it means that the battery is charging.

In order to prevent the battery degradation and ensure its longevity. The following constraint must be satisfied

$$SOC_b^{min} \leq SOC_b(k) \leq SOC_b^{max}. \quad (2)$$

where  $SOC_b^{min}$  and  $SOC_b^{max}$  represents the minimum and maximum allowable state of charge respectively. In addition, the battery has both a maximum power output  $P_b^{max}$  and a minimum power absorption capacity  $P_b^{min}$ , i.e.,

$$P_b^{min} \leq P_b(k) \leq P_b^{max}. \quad (3)$$

Finally, we associate to the battery the following cost function which is the sum of three terms evaluated over a time horizon of length  $T_H$

$$C_b = C_{b1} + C_{b2} + C_{b3} \quad (4)$$

with

$$C_{b1} = w_1 \sum_{j=0}^{T_H} P_b^2(j) \quad (5)$$

$$C_{b2} = w_2 \sum_{j=0}^{T_H} (SOC_b(j) - SOC_{opt})^2 \quad (6)$$

$$C_{b3} = w_3 \sum_{j=0}^{T_H} (P_b(j) - \frac{1}{T_H} \sum_{j=0}^{T_H} P_b(j))^2 \quad (7)$$

where

- $w_1$ ,  $w_2$  and  $w_3$  are weighting factors that assign varying levels of importance to the distinct terms.

- $C_{b1}$  signifies the cost linked to battery utilization, whether in charging or discharging mode. By applying a cost each time the battery is used, the system incentivizes exploring alternative energy sources. This approach aims to balance necessary battery usage while extending its lifespan and reducing expenses.
- $C_{b2}$  represents the cost of deviating from the optimal state of charge ( $SOC_{b,Opt}$ ) for the battery. Keeping the battery close to this level enables rapid power discharge or absorption, ensuring a significant margin for quick adjustments.
- $C_{b3}$  signifies the cost associated with battery behavior. To maximize performance and lifespan, it's crucial to minimize excessive charging and discharging cycles, known as "cycling".

### B. EV Model

The batteries of the EVs have the same characteristics of the battery of the charging station. EVs are capable of both absorbing and supplying power to the network, which is known as bidirectional capabilities or vehicle to grid (V2G) technology. If the power of EV  $P_{EV,i}(k)$  is negative then the  $i$ -th EV is providing energy, otherwise if  $P_{EV,i}$  is positive then the  $i$ -th EV is charging the battery. Similarly to the previous subsection we can write the dynamics also in terms of the state of charge  $SOC_{EV,i}$ , i.e.,

$$SOC_{EV,i}(k+1) = SOC_{EV,i}(k) + P_{EV,i}(k)T_s/E_{EV,i}^{max} \quad (8)$$

where  $E_{EV,i}^{max}$  is the maximum energy capacity. Moreover we introduce the following physical constraints

$$SOC_{EV,i}^{min} \leq SOC_{EV,i}(k) \leq SOC_{EV,i}^{max}, \quad (9)$$

and

$$P_{EV,i}^{min} \leq P_{EV,i}(k) \leq P_{EV,i}^{max} \quad (10)$$

where the meaning of the quantities  $SOC_{EV,i}^{min}$ ,  $SOC_{EV,i}^{max}$ ,  $P_{EV,i}^{min}$  and  $P_{EV,i}^{max}$ , is the same of the quantities  $SOC_b^{min}$ ,  $SOC_b^{max}$ ,  $P_b^{min}$ ,  $P_b^{max}$  but referred to the battery of the  $i$ -th EV.

We introduce now other quantities related to the  $i$ -th EV that will play an important role in the control methodology we propose. First, let  $t_{arr,i}$  and  $t_{dep,i}$  be, respectively, the arrival and departure time of the  $i$ -th EV at the charging station. It is worth observing that  $P_{EV,i}$  will be equal to 0 outside of the time interval  $[t_{arr,i}, t_{dep,i}]$ , that is,

$$P_{EV,i}(k) = 0 \text{ if } kT_s \notin [t_{arr,i}, t_{dep,i}].$$

Second let  $SOC_{init,i}$  be the state of charge in the  $i$ -th EV at its arrival time  $t_{arr,i}$  and let  $SOC_{req,i}$  be the state of charge which is required to be at the departure time  $t_{dep,i}$ . Finally let  $Flx_i$  be a flexibility index, which is a percentage of how much the owner of the  $i$ -th EV is flexible about its state of charge at departure time. Specifically, the energy stored by the battery of the  $i$ -th vehicle at the departure time, i.e.,  $SOC_{EV,i}(t_{dep,i})$ , has to satisfy the following relaxed constraint

$$(1 - Flx_i)SOC_{req,i} \leq SOC_{EV,i}(t_{dep,i}) \leq SOC_{req,i}. \quad (11)$$

We conclude this subsection by introducing the cost function  $C_{EV}$  associated to the EVs. This cost function depends on how much the owners of the EVs are satisfied. Specifically we have that

$$C_{EV} = w_4 \sum_{i=1}^{N_{EV}} (SOC_{EV,i}(t_{dep,i}) - SOC_{req,i})^2, \quad (12)$$

where  $N_{EV}$  is the total number of EVs arrived in the time horizon  $T_H$  and where  $w_4$  is a weighting factor expressing in the overall cost to be minimized the degree of interest in achieving the desired energy level of EVs.

### C. PV Model

We assume that PV source of the charging station always operates at its maximum power mode.

PV power generation prediction often involves uncertainties derived from weather forecasts. To address this, we propose a heuristic method based on real-time production data to update the expected power generation for the remaining day. Given a prediction horizon  $[0, T_H]$ , denoted by  $\hat{P}_{PV}(0), \dots, \hat{P}_{PV}(T_H - 1)$ , where  $\hat{P}_{PV}(k)$  represents expected power produced within  $[kT_s, (k+1)T_s]$ , and at the  $k$ -th sampling time, actual PV production values up to  $k$ ,  $P_{PV}(0), P_{PV}(1), \dots, P_{PV}(k)$ , are gathered, potentially differing from predictions. We propose to update the expected PV power production as

$$\hat{P}_{PV}^+(h) = \frac{\sum_{j=0}^k P_{PV}(j)}{\sum_{j=0}^k \hat{P}_{PV}(j)} \hat{P}_{PV}(h) \quad (13)$$

where  $\hat{P}_{PV}^+(h)$  is the updated version of  $\hat{P}_{PV}$  at the  $h$ -th sampling time.

### D. Grid Model

The cost of power from the grid refers to the monetary expense associated with drawing electricity from the utility grid to meet the energy demand.

The grid typically has limitations on the minimum and maximum power that can be exchanged with the network. These constraints are important to ensure the stability and reliability of the grid system. We assume that

$$P_g^{min} \leq P_g(k) \leq P_g^{max} \quad (14)$$

where  $P_g(k)$  is the power exchanged between the grid and the station and it can be negative or positive. When it is negative the grid is buying energy, when it is positive the grid is selling energy. The cost function associated with the grid is

$$C_g = \sum_{j=0}^{T_H} w_5 P_g(j), \quad (15)$$

where  $w_5$  is a weighting factor that, for simplicity, is assumed to be constant.

The extension to time-varying scenarios will be the subject of future investigation.

## III. MPC-BASED CENTRALISED POWER CONTROL DESIGN

Our optimization problem involves making decisions regarding how to distribute energy resources over the upcoming day. The goal is to minimize costs while also ensuring a consistent and reliable energy supply. In our study, it is not necessary to update the control decisions every minute at the start of the day when there is neither PV production nor any EVs plugged in. However, as soon as EVs begin to arrive or the PV system initiates power generation, the control decisions need to be promptly updated.

### A. Optimization Problem Methodology

In our setup we aim at minimizing the cost function

$$C_{Tot} = C_b + C_g + C_{EV}$$

where  $C_b, C_g, C_{EV}$  are defined as in (4), (15) and (12), respectively, by regulating the power flows between the EVs, the grid, the battery and the PV. We assume the optimization problem is defined over one day. Let  $t_0$  and  $t_f$  be the initial and final time instants, respectively. Then  $t_f - t_0 = 24$  hours. It is convenient to assume that  $t_0$  is midnight and, hence,  $t_f$  is the midnight of the day after. Moreover, accordingly to the description provided in the previous section, we assume the control actions are discretized by the sampling time  $T_s$ . Let  $T_H$  denote the total number of time slots, that is,  $T_H = (t_{fin} - t_{init})/T_s$ .

The optimization problem we consider is split into two phases. To define them we introduce  $t_{start} = \bar{k}T_s$ , which is the time instant when either real EVs start to arrive or the PV starts to produce. The first phase refers to the optimization over the interval  $[t_0, t_{start}]$ , while the second phase over the interval  $[t_{start}, t_f]$ , see Figure 1.

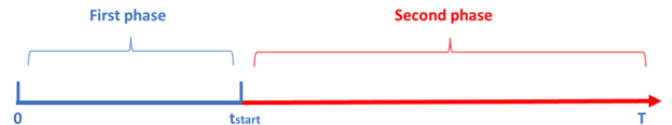


Fig. 1: The two phases of the optimization problem.

Let us consider the first phase. We assume that the information available at time  $t_0$  is

- Expected PV production for the day ahead, that is,  $\hat{P}_{PV}(0), \hat{P}_{PV}(1), \dots, \hat{P}_{PV}(T_H - 1)$ .
- The state of the charge of the battery.
- A prediction on the EVs which will arrive in the entire interval  $[t_0, t_f]$ . This information is formally described by the set

$$\hat{S} = \left\{ \hat{D}_1, \hat{D}_2, \dots, \hat{D}_{\hat{N}_{EV}} \right\}$$

where

$$\hat{D}_i = \left\{ \hat{S}\hat{O}C_{init,i}, \hat{S}\hat{O}C_{req,i}, \hat{t}_{arr,i}, \hat{t}_{dep,i}, \hat{F}\hat{l}x_i \right\}$$

being

- $\hat{N}_{EV}$  the expected number of vehicles arriving in  $[t_0, t_f]$ ;
- $\hat{t}_{arr,i}, \hat{t}_{dep,i}$  the expected arrival and departure times, respectively, of the  $i$ -th expected vehicle;
- $\hat{E}_{init,i}$  the expected initial energy stored in the  $i$ -th EV at its arrival time.
- $\hat{E}_{req,i}$  the expected required energy of the  $i$ -th EV at the departure time.
- $\hat{Flx}_i$  the expected flexibility index of the  $i$ -th EV.

The information in  $\hat{S}$  can be obtained employing a prediction model based on historical data. We will discuss how to generate  $\hat{S}$  in next section.

At time  $t_0$  the following optimization problem is solved

$$\min_{u(0), \dots, u(T_H-1)} C_{Tot}$$

where  $u(j) = \{P_g(j), P_b(j), P_{EV,i}(j), i = 1, \dots, \hat{N}_{EV}\}$ , subject to the dynamics of the battery in (1), the dynamics of the vehicles in (8), the physical constraints in (2), (3), (9), (10), the energy requirements in (11) and the power balance of the network

$$P_b(j) + \sum_{i=1}^{\hat{N}_{EV}} P_{EV,i}(j) = P_g(j) + \hat{P}_{pv}(j) \quad (16)$$

for all  $j \in [0, T_H - 1]$ . This phase determines initial control decisions, such as charging the battery before high power demand coincides with EV arrivals or discharging it to capture surplus PV energy. By solving a single optimization problem at time  $t_0$ , considering predicted EV arrivals and departures, individual EV energy requirements, and forecasted PV production, control inputs are determined and applied until the first EV arrives or PV generation begins. Therefore no other optimization problems are solved before the time instant  $t_{start} = \bar{k}T_s$  and the control inputs  $u(0), u(1), \dots, u(\bar{k}-1)$ , calculated solving the optimization problem at time  $t_0$ , are applied within the interval  $[t_0, t_{start}]$ .

Now let us consider the second phase. We start by observing that at time  $t_f$ , based on the EVs that actually arrived at the station, we can define the set of real data

$$S = \{D_1, D_2, \dots, D_{N_{EV}}\}$$

where  $N_{EV}$  is the number of vehicles actually arrived in  $[t_0, t_f]$  and where

$$D_i = \{SOC_{init,i}, SOC_{req,i}, t_{arr,i}, t_{dep,i}, Flx_i\},$$

being  $SOC_{init,i}, SOC_{req,i}, t_{arr,i}, t_{dep,i}, Flx_i$  the real data associated to the  $i$ -th vehicle.

We assume that, once the  $i$ -th real EV arrives at the charging station it directly communicates the information about its state of charge, the departure time and the corresponding energy required at this time.

Now suppose that we are at time  $kT_s$  for  $k \geq \bar{k}$ , that is  $t_{start} \leq kT_s \leq t_f$ . Observe that, in the second phase the optimization problem must take into consideration also the available real data. To do that, it is convenient to split both

the expected data set  $\hat{S}$  and the real data set  $S$  into two subsets as follows

$$\hat{S}_k^- = \{\hat{D}_i \in \hat{S} | \hat{t}_{arr,i} \leq kT_s\}, \hat{S}_k^+ = \{\hat{D}_i \in \hat{S} | \hat{t}_{arr,i} > kT_s\}$$

$$S_k^- = \{D_i \in S | t_{arr,i} \leq kT_s\}, S_k^+ = \{D_i \in S | t_{arr,i} > kT_s\}.$$

Clearly  $\hat{S} = \hat{S}_k^- \cup \hat{S}_k^+$  and  $S = S_k^- \cup S_k^+$ . Notice also that real information contained in  $S_k^+$  refers to vehicles which will arrive after  $kT_s$  and, in turn, it can not be used in the optimization process. Based on this observation, we define the set

$$\bar{S}_k = S_k^- \cup \hat{S}_k^+,$$

containing the past and current real information related to vehicles that arrived before  $kT_s$  and the information about the vehicles which are expected to arrive in  $[kT_s, t_f]$ . For convenience let  $\mathcal{N}_{\bar{S}_k}$  be the set of real and expected vehicles whose information is contained in  $\bar{S}_k$ .

The optimization at  $kT_s$  is performed over  $\bar{S}_k$  and aims at minimizing the cost function

$$\min_{u(k), \dots, u(T_H-1)} C_{Tot}(k) = C_b(k) + C_g(k) + C_{EV}(k) \quad (17)$$

where

$$C_b(k) = \sum_{j=k}^{T_H} w_1 P_b^2(j) + w_2 (SOC_b(j) - SOC_{opt})^2$$

$$+ w_3 (P_b(j) - \frac{1}{T_H} \sum_{j=k}^T P_b(j))^2$$

$$C_{EV}(k) = w_4 \sum_{i \in \mathcal{N}_{\bar{S}_k}} (SOC_{EV,i}(t_{dep,i}) - SOC_{dep,i})^2$$

$$C_g(k) = w_5 \sum_{j=k}^{T_H} P_g(j)$$

subject to the dynamics of the battery in (1), the dynamics of the vehicles in (8), the physical constraints in (2), (3), (9), (10), the energy requirements in (11) and the power balance of the network in (16), where the expected PV production is updated using the heuristic in (13).

At time  $kT_s$  only the first input of the sequence  $u(k), u(k+1), \dots, u(T_H-1)$  calculated by solving the above problem, that is  $u(k)$ , is applied. At time  $(k+1)T_s$ , the optimization problem is reformulated based on the actual PV power injected and on the real information of new vehicles that just arrived. These iterations are performed until final time  $t_f$ .

## B. Arrival Modelling

In this section, we explain how we model the arrival of the vehicles and how we generate the information within the set  $\hat{S}$ . In particular we describe the synthetic data generator (SDG) we use to determine  $\hat{N}_{EV}$  and, in turn, the data  $\hat{D}_i$ ,  $i = 1, \dots, \hat{N}_{EV}$ . In this work, we assume the arrival pattern is modelled in a probabilistic way by pairing Poisson distributions with uniform distributions. For example, if we

are interested in understanding how many vehicles arrive at a specific location within an hour, the Poisson distribution can provide the likelihood of different arrival counts based on historical data. The uniform distribution ensures that events, in this case vehicles arrivals, occur at random times within a fixed interval. By combining these distributions, we can generate a realistic model of vehicles arrival which allows us to make informed predictions about the number of vehicles and their arrival times.

1) *Arrival Count Model:* We divide the time horizon  $[t_0, t_f]$  into time slots of length  $\Delta t$ . Consider the  $h$ -th time slot, that is  $[t_0 + (h - 1)\Delta t, t_0 + h\Delta t]$ , and let  $N_h$  be the number of EVs arriving within it. Then  $N_h$  is modeled as a Poisson distribution of parameter  $\lambda_h$ , that is, given a nonnegative integer number  $K$ , the probability that  $K$  EVs will arrive during the  $h$ -th time slot is

$$P(N_h = K) = \frac{e^{-\lambda_h} \lambda_h^K}{K!}, K = 0, 1, 2, \dots \quad (18)$$

The parameter  $\lambda_h$  represents the average rate of EVs arrival during the  $h$ -th slot and can be estimated based on some historical data.

Now let us assume that for each  $h = 1, 2, \dots, N_\Delta$  ( $N_\Delta$  represents the total number of time slots), the corresponding value of  $\lambda_h$  has been assigned. Then the estimated number  $\hat{N}_h$  of EVs arriving during the  $h$ -th slot is obtained by sampling the corresponding Poisson distribution. It turns out that the total number  $\hat{N}_{EV}$  of EVs expected to arrive within  $[t_0, t_f]$  is given by  $\hat{N}_{EV} = \sum_{h=1}^{N_\Delta} \hat{N}_h$ .

2) *Arrival Times Model:* For  $i = 1, \dots, \hat{N}_{EV}$ , assume that the  $i$ -th EV is expected to arrive within the  $h$ -th time slot. Then, the corresponding  $\hat{t}_{arr,i}$  is predicted as follows. Let us generate  $\bar{t}_i$  by sampling the uniform distribution in  $[0, \Delta t]$ . Then

$$\hat{t}_{arr,i} = (h - 1)\Delta t + \bar{t}_i.$$

3) *Energy required model:* The energy required is generated randomly as follows. We are interested into the case where EVs arrive to the station with a low energy. Let  $E_H$  be a certain high energy level (for example we can set  $E_H = 0.7E_{EV}^{max}$ ). The the expected required energy  $\hat{E}_{req,i}$  for  $i = 1, \dots, \hat{N}_{EV}$  is generated randomly around the level ( $E_H$ ) using uniform distribution

$$\hat{E}_{req,i} \sim U[(1 - c)E_H, (1 + c)E_H] \quad (19)$$

where parameter  $c$  can be estimated based on historical data. In our setup we assume  $c = 0.1$ .

4) *Departure time model:* We consider a specific scenario in which the EVs will stay at the station for a long period. Depending on the capacity and the maximum power of the EV's battery, we can calculate the minimum necessary time  $t_{min}$  to fully charge the EV battery. We set the connection time  $\hat{t}_{c,i}$  of the  $i$ th EV to be greater than this period and to be less than a maximum time  $t_{max} = t_{min} + b$ , where also parameter  $b$  can be estimated from historical data. In our setup we assume  $b = 1$  hour.

$$\hat{t}_{c,i} \sim U[t_{min}, t_{max}] \quad (20)$$

The time of departure  $\hat{t}_{dep,i}$  can be calculated as follows:

$$\hat{t}_{dep,i} = \hat{t}_{arr,i} + \hat{t}_{c,i} \quad (21)$$

#### IV. NUMERICAL RESULTS

In this section we provide simulation results to demonstrate the effectiveness of the proposed control approach. In particular we compare the MPC solution described in Section III with an heuristic method where the connected EVs tend to charge at maximum power rate if the available power is enough. In this heuristic solution, we can face with different cases. If the power of PV is greater than the power demand then we assume the surplus energy goes to the battery or to the grid if the battery is fully charged. When the power of PV is not enough, the first support to the EVs comes from the battery. If the sum of the PV power and the battery power is not enough, then grid will provide additional power to the EV. The last case is when the sum of all power sources is not enough; the available energy will be dispatched and divided through the connected EVs equally.

##### A. System Parameters

The parameters of the system are summarized in tables I, II. We set the maximum power that can the grid provides to the network to  $P_g^{max} = 100KW$  and the minimum power to  $P_g^{min} = -100KW$ . The PV data are taken from IEEE PES (Power And Energy Society) for two different days as shown in Figure 2. The expected PV power for one day ahead is configured for optimal sunlight conditions (red line). The real PV power is configured for a cloudy day (blue line).

$E_{EV,i}^{max}$	$E_{EV,i}^{min}$	$SOC_{EV,i}^{max}$	$SOC_{EV,i}^{min}$	$P_{EV,i}^{max}$
40 KWh	0 KWh	1	0	14 KW
$P_{EV,i}^{min}$	$flx_i$	$t_{min}$	$t_{max}$	$SOC_H$
-14 KW	10 %	300 min	360 min	0.7

TABLE I: EVs battery parameters and constraints

$E_b^{max}$	$E_b^{min}$	$SOC_b^{max}$	$SOC_b^{min}$
400 KWh	80 KWh	1	0.2
$P_b^{max}$	$P_b^{min}$	$E_{b,Opt}$	$SOC_{b,Opt}$
60 KW	-60 KW	200 KWh	0.5

TABLE II: ESS battery parameters and its constraints

$h$	7	8	9	10	11	12	13	14	15	16	17	18
$\lambda_h$	2	3	5	6	7	8	7	6	5	4	3	2

TABLE III: Rate of the EVs arrival with the Poisson distribution model

The simulation time is 24 hours, with sampling time  $T_s = 1.5$  min. The time interval  $\Delta t$  is equal to 1 hour. In Table III, we report the values of  $\lambda_h$  for different time slots ( $\lambda_h = 0$  for  $h < 7$  and  $h > 18$ ). The peak hours have

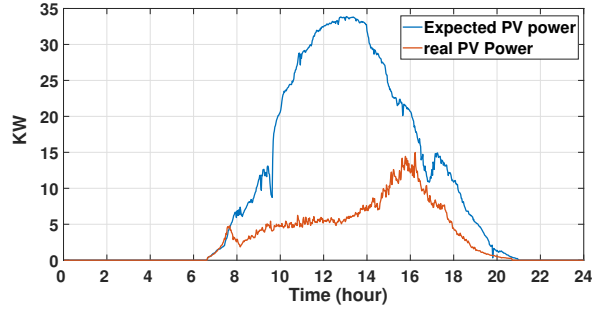


Fig. 2: The expected PV power production: blue line, the real PV power production: red line

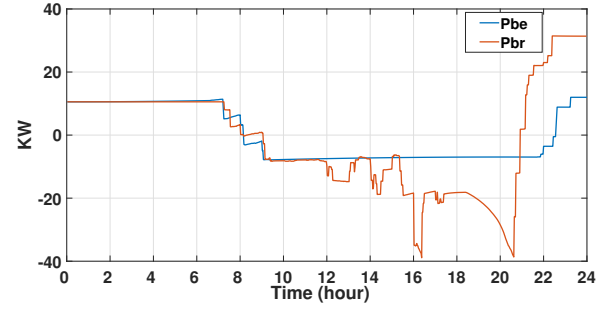


Fig. 4: The expected power of the battery: blue line vs its real power during the day: red line

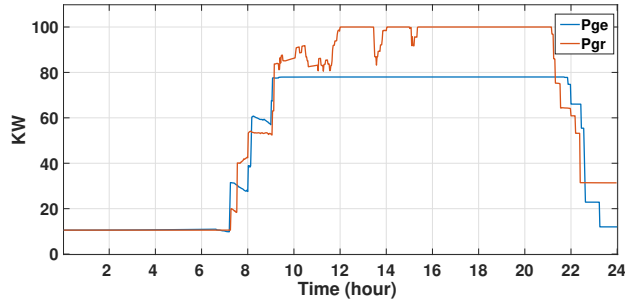


Fig. 3: The expected power of the grid: blue line vs its real power during the day: red line

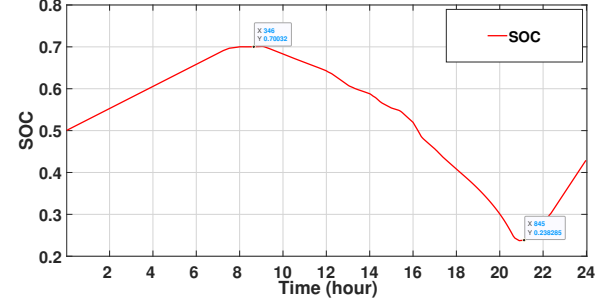


Fig. 5: The state of charge of the battery.

greater average (8 EVs per hour), while other times have less average (2 EVs per hour).

We set  $P_b^{max} = 14kW$  since 88% of charging points are between  $7.4kW$  and  $22kW$ . The minimum  $SOC$  is 20% and maximum  $SOC$  is 100%.

Concerning the generation of the data inside  $\hat{S}$ , we use the synthetic data generator described in section III. In particular the required energy for each expected EV has been generated between  $22KWh$  and  $32KWh$ . Concerning the real data, since the simulation is done online as test, not in real environment, we use the same synthetic data generator to generate also a sample for real EVs. In our test we have that  $\hat{N}_{EV} = 56$  and  $N_{EV} = 60$ . Moreover  $t_{start} = 6.65 h = 399 min$  or  $\bar{k} = 266$ .

### B. Grid and Battery Power Performance

Figure ( 3, 4) describes a graphical representation of the power of the grid and battery, respectively, with blue and red lines indicating the expected and real power, respectively. The expected behavior refers to the one computed solving the optimization problem of the first phase at time  $t_0$ .

The deviation of the real power from the expected one is due to the difference between the real PV production and the expected one, and to the difference between the expected arrival EVs and real arrival EVs. One can see that the battery has discharged more than expected, because of the higher power demand of EVs and lower PV real power production. Initially at the start of the day without any EVs, the battery undergoes a smooth charging process. As the

EVs begin to arrive and the actual PV power falls short, the battery is utilized to compensate for the energy deficit, leading to discharge down to 0.23 as shown in Figure 5. Towards the end of the day, the battery enters a recharging phase.

### C. Performance on EV Charging Coordination

Figure 6 and 7 illustrate the charging power rate for both methods for EVs samples that arrive at the beginning of the day ( $EV_1, EV_2, EV_6$ ) and that arrive during a high-demand period within a day ( $EV_{20}, EV_{25}, EV_{30}$ ). We made the assumption that there is not a significant demand at the charging station during the beginning of the day. In MPC method, as the EVs get connected for charging, the station initiates the charging process at the highest power flow possible. Subsequently, during the peak hours, the EVs that arrive first function as an energy storage system, effectively compensating for the power shortages. The charging rate varies from one EV to another, based on individual requirements. Whereas in the heuristic method, the power available in the network is dispatched equally to all connected EVs, also it is clear that there is no benefits from EVs since V2G is not used. That lead to a mal manamengent of the energy which results on dissatisfaction of consumer where EV energy requirements are not achieved. This fact is highlighted in Figures 8 and 9 reporting the behavior of the state of charge for EVs and in Table IV.

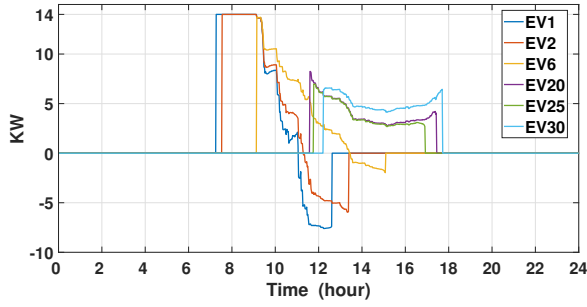


Fig. 6: The EVs charging rate using MPC method

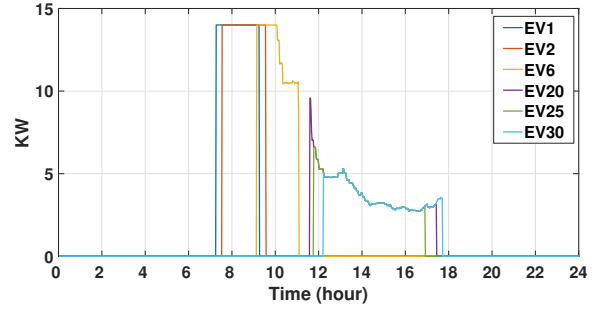


Fig. 7: The EVs charging rate using heuristic method

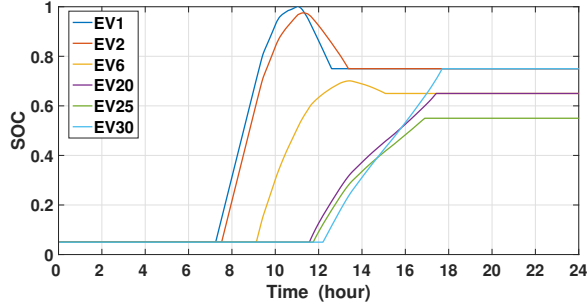


Fig. 8: The SOC of different EVs using MPC

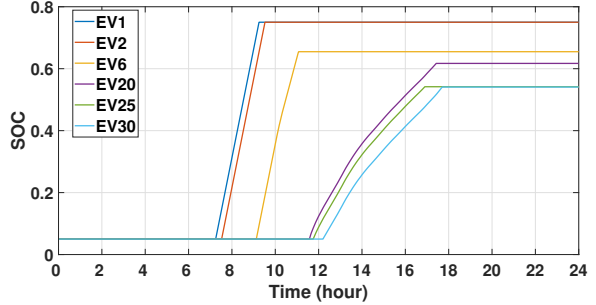


Fig. 9: The SOC of different EVs using heuristic method

	EV <sub>1</sub>	EV <sub>2</sub>	EV <sub>6</sub>	EV <sub>20</sub>	EV <sub>25</sub>	EV <sub>30</sub>
$SOC_{req,i}$	0.75	0.75	0.65	0.65	0.55	0.75
$SOC_{dep,i}$ (MPC)	0.75	0.75	0.65	0.65	0.55	0.75
$SOC_{dep,i}$ (Heuristic)	0.75	0.75	0.65	0.61	0.54	0.54

TABLE IV: The required SOC and the SOC at departure time using MPC and heuristic methods for samples of EVs.

More precisely, as illustrated in Table IV, one can see that using the MPC method developed in this paper, all EVs have the required SOC at the departure times, whereas using the heuristic method, the EVs which arrived at the peak period time do not reach the required SOC at the departure time.

## V. CONCLUSIONS

In conclusion, the implementation of the MPC-based centralized power control in a power charging station system with ESS battery and PV coordination offers several significant advantages and outcomes.

The model used was based on the expected information about EVs; in addition, when the real EV is plugged in, the owner provides important parameters, in particular the required energy at its departure time. Adding these data in this framework, ensures efficient utilization of resources as we have seen in our numerical test.

Despite the benefits, challenges includes accurate prediction of PV generation, EV mobility patterns, and the need for real-time data communication. As future work, we intend to implement this method in real environment.

## REFERENCES

[1] O. Erdinc, N. G. Paterakis, T. D. Mendes, A. G. Bakirtzis, and J. P. Catalão, "Smart household operation considering bi-directional ev and ess utilization by real-time pricing-based dr," *IEEE Transactions on Smart Grid*, vol. 6, no. 3, pp. 1281–1291, 2014.

[2] W. Tushar, C. Yuen, S. Huang, D. B. Smith, and H. V. Poor, "Cost minimization of charging stations with photovoltaics: An approach with ev classification," *IEEE Transactions on Intelligent Transportation Systems*, vol. 17, no. 1, pp. 156–169, 2015.

[3] G. Perin, F. Meneghello, R. Carli, L. Schenato, and M. Rossi, "Ease: Energy-aware job scheduling for vehicular edge networks with renewable energy resources," *IEEE Transactions on Green Communications and Networking*, vol. 7, no. 1, pp. 339–353, 2022.

[4] L. Jian, H. Xue, G. Xu, X. Zhu, D. Zhao, and Z. Shao, "Regulated charging of plug-in hybrid electric vehicles for minimizing load variance in household smart microgrid," *IEEE Transactions on Industrial Electronics*, vol. 60, no. 8, pp. 3218–3226, 2012.

[5] L. Wang, Z. Qin, T. Slangen, P. Bauer, and T. Van Wijk, "Grid impact of electric vehicle fast charging stations: Trends, standards, issues and mitigation measures-an overview," *IEEE Open Journal of Power Electronics*, vol. 2, pp. 56–74, 2021.

[6] A. Nursimulu, "Demand-side flexibility for energy transitions: ensuring the competitive development of demand response options," *International Risk Governance Council, Report*, 2015.

[7] F. Simmini, M. Agostini, M. Coppo, T. Caldognetto, A. Cervi, F. Lain, R. Carli, R. Turri, and P. Tenti, "Leveraging demand flexibility by exploiting prosumer response to price signals in microgrids," *Energies*, vol. 13, no. 12, p. 3078, 2020.

[8] S. Suraj and K. Senthil, *Demand side management: demand response, intelligent energy systems and smart loads*. SSRN, 2020.

[9] W. Kong, F. Luo, Y. Jia, Z. Y. Dong, and J. Liu, "Benefits of home energy storage utilization: An australian case study of demand charge practices in residential sector," *IEEE Transactions on Smart Grid*, vol. 12, no. 4, pp. 3086–3096, 2021.

[10] F. Simmini, T. Caldognetto, M. Bruschetta, E. Mion, and R. Carli, "Model predictive control for efficient management of energy resources in smart buildings," *Energies*, vol. 14, no. 18, p. 5592, 2021.

[11] S. R. Cominesi, M. Farina, L. Giullioni, B. Picasso, and R. Scattolini, "A two-layer stochastic model predictive control scheme for microgrids," *IEEE Transactions on Control Systems Technology*, vol. 26, no. 1, pp. 1–13, 2017.

[12] A. Parisio, E. Rikos, and L. Glielmo, "Stochastic model predictive control for economic/environmental operation management of microgrids: An experimental case study," *Journal of Process Control*, vol. 43, pp. 24–37, 2016.